SEGMENTATION SCHEMES FOR PRIMARY AND SECONDARY MIRRORS OF THE SCHWARZSCHILD-COUDER TELESCOPE FOR CTA

Author	*Laboratory*
Julien Rousselle	**UCLA**
Vladimir Vassiliev	**UCLA**

Approved by	*Laboratory*

List of Abbreviations			
SCT	Schwarzchild-Couder Telescope		
SC	Schwarzchild-Couder		
OS	Optical System		
FoV	Field of View		

History		
Version	Date	Observation

Distribution	SCT group

- Table of Contents -

1.1 Introduction

This memo provides several possible designs for the primary and secondary mirror segmentations of the Schwarzschild-Couder (SC) telescope. These designs are the result of an optimization to reduce the size and the number of mirror segments. Optimization is performed with additional constraints imposed by the mirror fabrication technologies.

The segmentation schemes described were developed for the baseline SCT design for CTA with a field of view (FoV) of 8 deg and a focal length of 5.5863 m as described in the memo "Optical systems of Schwarzschild-Couder Telescope for CTA" (Ref…). These segmentations are provided in order to enable discussion of the segmentation schemes for the primary and secondary mirrors with the goal to arrive to a final decision on the segmentation scheme for SCT optical system (OS), which is necessary for the development of the SCT alignment system and mechanical system designs.

1.2 Definition

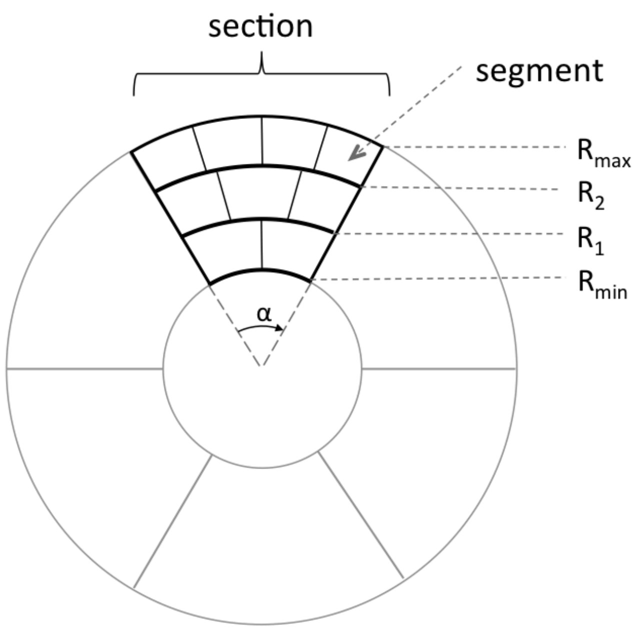

Figure 1: Explanation of the terms used in this memo with an example of segmentation.

The SCT primary and secondary mirrors are made by the repetition of identical sections (Fig. 1) composed of "petal" segments on 2 or 3 rings. The section is defined by the angle $\alpha=360^{\circ}/n$ with n an integer and the segments are defined by the ring radii (R_1,R_2) and the number of segments on each ring.

The minimum and maximum radii of the mirrors in the SCT OS are:

Primary Mirror $\quad R_{min}=2.1933\ m$

$R_{max}=4.8319\ m$

Secondary Mirror $\quad R_{min}=0.3945\ m$

$$R_{max} = 2.7083\ m$$

1.3 Primary mirror segmentations

1.3.1 *Design optimization*

The first constrain for the segmentation designs was the technical capability of the industry to produce large mirrors. The limited size of the industrial tools required for fabrication of mandrels and mirrors impose a constraint on the largest dimension of the petal segment, its diagonal. Thus, the simulation program was developed to study and qualify the different designs using the segment diagonal as an input. The objective was to minimize the number of segments, to reduce the mirror cost and complexity, and to maximize the segment area for a given diagonal, in the range 1.2 - 2 meters. Starting from the outer ring, we calculated the maximum segment area for a given diagonal and then the number of segments and the ring inner radius. The same process occurs for the middle ring whereas an adjustment of the diagonal is needed for the inner ring due to the limited remaining area. At the end we calculated how far the inner segment area is from the maximum (for the given diagonal) in order to select and rate the segmentation schemes. The advantage of this optimization is that there is no need of a segment distribution to start the process. The program is free to study every possible design fulfilling the requirements described above. The drawback is a variation of the segment diagonal and area in the inner ring.

A second independent optimization was developed, using a different approach. This program used a given segment distribution on the rings as input. For each distribution the segment diagonal and ring radii were calculated in order to obtain a constant segment diagonal and area. Then the distribution was rated by calculating how far the segment areas are from the maximum for a given diagonal. This optimization leads to a constant segment area and thus a constant reflection contribution but needs to know a priori every possible segment distribution before the optimization.

The results of the both optimizations were compared to select the best candidate segmentation schemes.

1.3.2 *Summary of the optimization results*

The figure 2 shows the total number of segments as a function of the segment diagonal for the ten best candidate segmentation schemes of the primary mirror, including a design made of only two rings (the last point). The number of segments in the primary appears to be approximately linearly dependent on the diagonal size even for a design with two rings. One segmentation scheme, which uses 60 segments and a diagonal of 1.4 meters, doesn’t follow this linearity trend and seems to be more compact than the other designs. This design, denoted "D" in the Table 1, is therefore the favorable candidate for the primary mirror segmentation with the three rings arrangement.

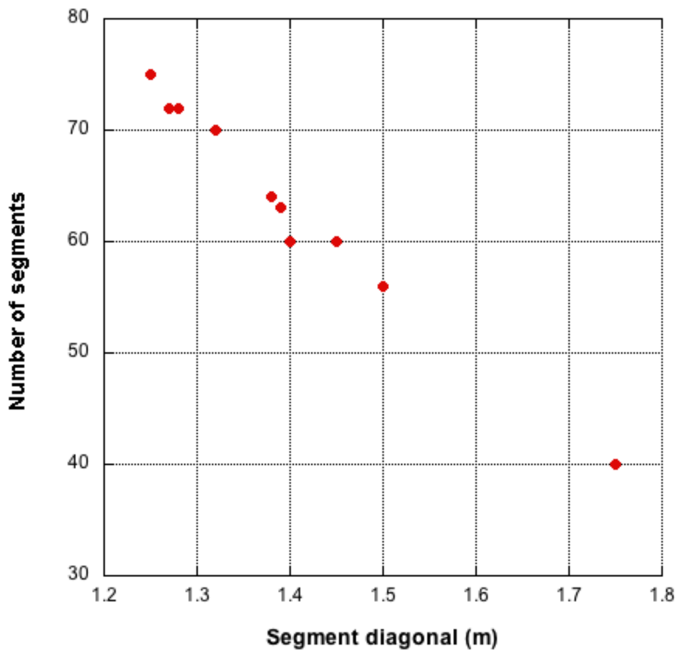

Figure 2: Total number of segments as a function of the segment diagonal for the ten best design candidates. The designs are made of three different rings, except the last one made of only two rings.

Table 1 summarizes the segmentation schemes for the primary mirror, including the fold symmetry, the total number of segments and their distributions.

ID	number of sections	α (deg)	total number of segments	number of segments per section P1	P2	P3	D (m)
A	5	72	75	4	5	6	1.25
B	6	60	72	3	4	5	1.26
C	8	45	72	2	3	4	1.27
D	5	72	60	3	4	5	1.40
E	8	45	40	2		3	1.75

Table 1: Definitions of the segmentation schemes for the primary mirror. It is made of 3 different rings, except the last one with only 2 rings. d is the maximum segment diagonal needed to produce the segmentation scheme. P1, P2, P3 are respectively the inner, middle and outer rings.

The both D and E segmentation schemes are shown in Figure 3 to illustrate the segment distribution and the fold symmetry.

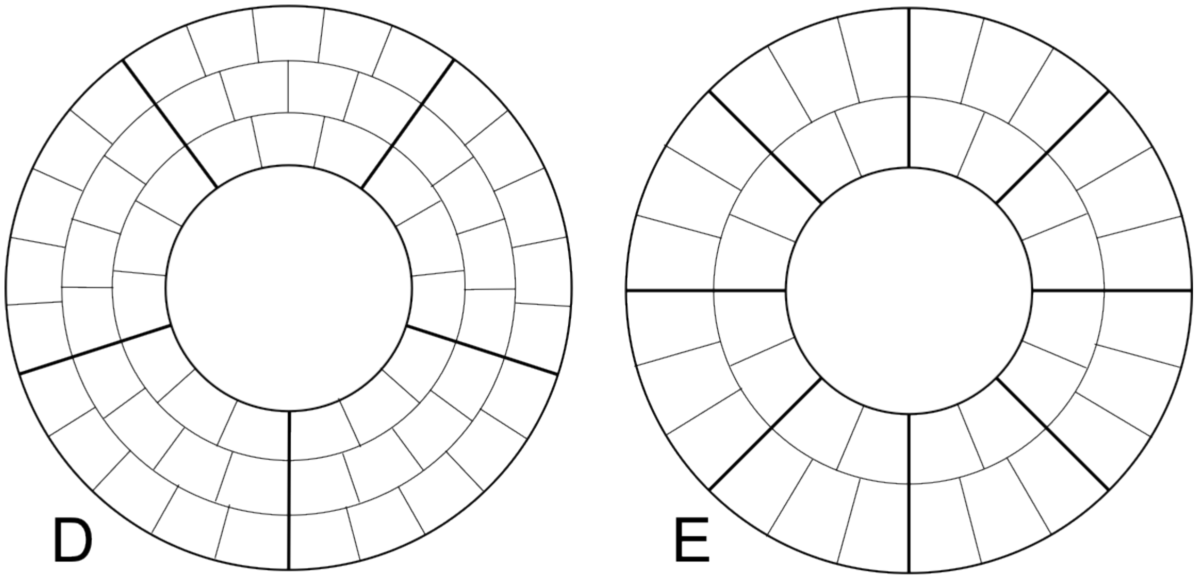

Figure 3: Representations of the D (left) and E (right) designs of the primary mirror which utilize 60 and 40 segments respectively distributed on 3 and 2 rings.

1.3.3 Additional constrains for hybrid glass mirrors

The use of thin glass sheets for the fabrication of mirrors through cold glass slumping process introduces new constraint due to the fragility of the glass. The cut of the thin glass sheet along a curved edge increases failure rate during slumping due to large number of small cracks appearing around such cut. A solution to this problem is to cut the flat glass sheet before slumping along a straight line, as close as possible to the ideal "petal" design.

If applied, this requirement introduces new segmentation schemes, with straight edges, as shown in Figure 4. From the inner to the outer ring, one can only multiply the number of segments by 1 or 2, in order to produce a continuous surface.

Another potential constrain comes from the size of the glass sheets available in the industry to produce the mirror segments. This size defines the largest bounding box allowed around the segments. A typical size of 1.25x1.45 m^2 was used to develop the segmentation of the hybrid glass mirrors shown in the next section. Nevertheless, one could overtake this constrain using larger and more expensive glass sheets, if needed.

1.3.4 Favorable segmentation schemes for the primary hybrid glass mirrors

The baseline segmentation scheme (F) for hybrid glass mirrors is made of 2 rings and 16 sections for a total of 48 segments. This design respects the constraints inherent to the thin glass sheets described in the previous section, using straight cuts (Figure 4) and bounding box smaller than the typical glass sheet size (1.25x1.45 m^2).

The applicability of the cold glass slumping technique has not yet been demonstrated for the aspheric mirrors of the SCT primary, although theoretical consideration of glass deformation suggest that this technology sholud be succesful. It is a possibility, however, that for the large size segments the sag of several millimiters may not be achievable in the slumping process especially for the inner ring with the largest curvature and deviation from conical surface. It is then possible to reduce the stress on the glass using smaller segments and a 3 rings segmentation scheme. Thus, a backup segmentation scheme (G) was developped, respecting the same constraints and using 13 sections for a total of 65 segments. This segmentation scheme may also have some advantage for three point support of the mirror segments due to being more close to the optimal relationship between segment diagonal and area. The disadvantage is the increased number of segments and consequent complexity and cost of alignment system.

ID	number of sections	α (deg)	total number of segments	number of segments per section			D (m)
				P1	P2	P3	
F*	16	22.5	48	1		2	1.64
G	13	28	65	1	2	2	1.41

Table 2: Definitions of the segmentation schemes for the primary mirror made of hybrid glass. d is the maximum segment diagonal needed to produce the segmentation scheme. P1, P2, P3 are respectively the inner, middle and outer rings. The star represents the default segmentation scheme.

The Figure 4 shows the both F and G segmentation schemes described in Table 2.

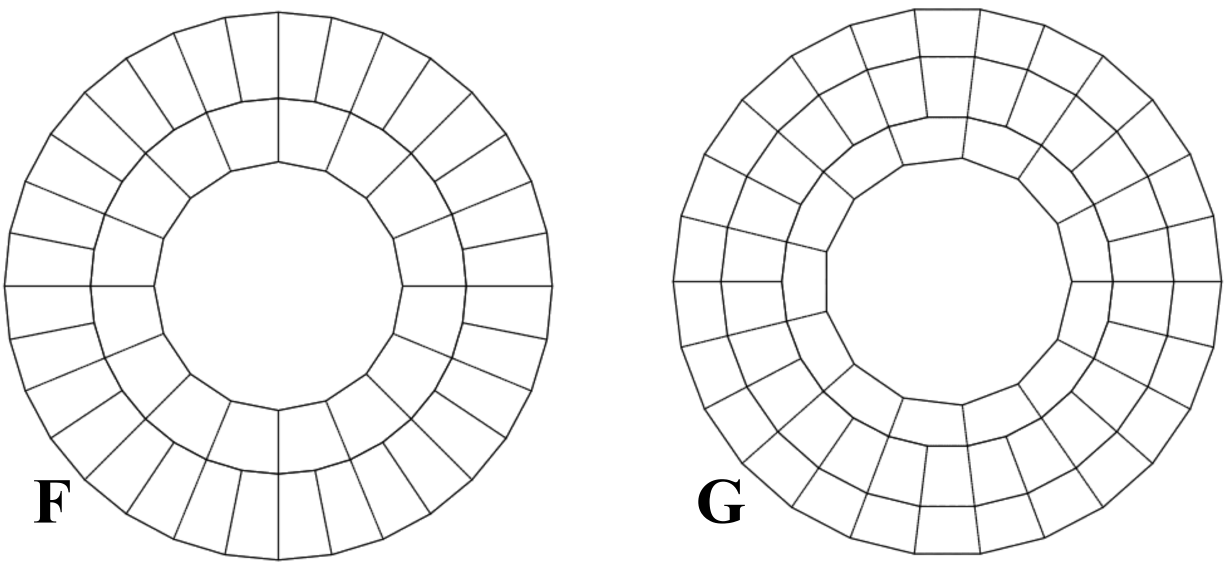

Figure 4: Representations of the F (left) and G (right) designs of the primary mirror, made of hybrid glass substrate with 48 and 65 segments respectively distributed on 2 and 3 rings.

1.4 Secondary mirror segmentation schemes

The secondary mirror segmentation was studied with the same technique used for the primary mirror and described in **Error! Reference source not found.**. Nevertheless, the smaller size of the mirror for the same range of segment diagonal leads to a fewer number of design options.

Table 2 summarizes the segmentation schemes for the secondary mirror, including the fold symmetry, the total number of segments and their distributions.

ID	number of sections	α (deg)	total number of segments	number of segments per section			D (m)
				S1	S2	S3	
H	4	45	36	2	3	4	1.15
I	5	72	30	1	2	3	1.26
J*	8	45	24	1		2	1.38
K	5	72	20	1		3	1.47

Table 2: Definitions of the segmentation schemes for the secondary mirror. It can be made of 3 or 2 different rings. d is the maximum segment diagonal needed to produce the segmentation scheme. S1, S2, S3 are respectively the inner, middle and outer rings. The star represents the default segmentation scheme.

The both I and J segmentation schemes are shown Figure **Error! Reference source not found.** to give an idea of the segment distribution and the fold symmetry.

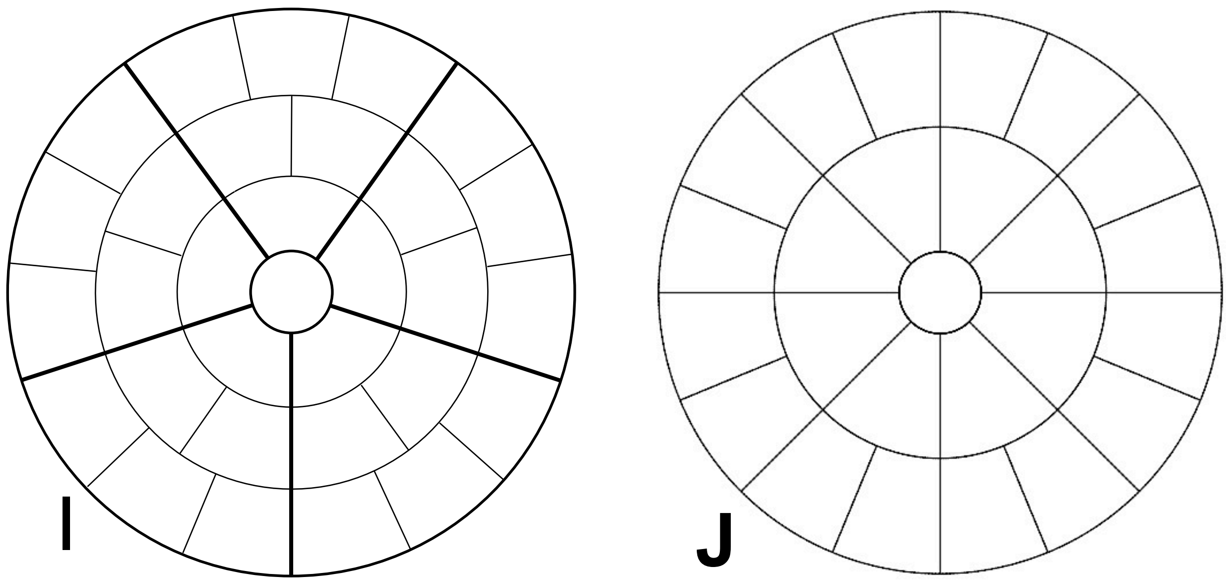

Figure 5: Representations of the G (left) and H (right) designs of the secondary mirror. They use respectively 30 and 24 segments distributed on 3 and 2 rings.

1.4.1 Secondary mirror made of hybrid glass substrate

If for any reason the secondary segments can't be produced using electroforming, a backup segmentation was developed using hybrid glass mirrors, with the associated constrains exposed in section 1.3.3.
This segmentation scheme, presented Figure 6, is derived from the default J design with straight edges

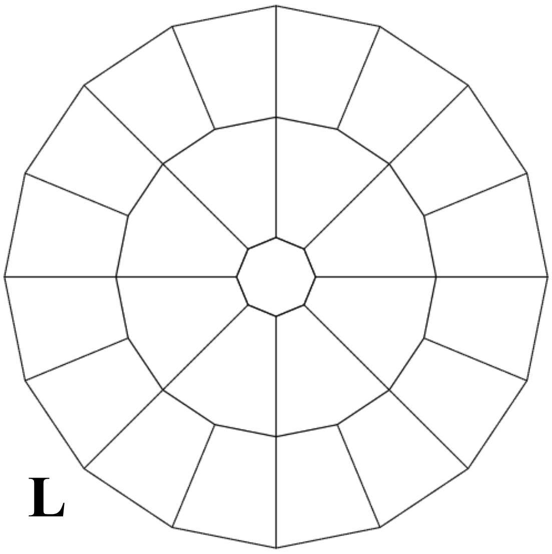

Figure 6: Representations of the L design of the secondary hybrid glass mirror. It uses 24 segments distributed on 2 rings.

1.5 Segment parameters for the default F and J segmentation schemes

The Tables 3 and 4 describe respectively the segment parameters from the F and J favorite segmentation schemes, presented in Figure 4 and 5.

Mirror ring	P1	P2
Number of segments	16	32
φ_{min} (deg)	-11.25	-5.62
φ_{max} (deg)	11.25	5.62
R_{min} (m)	2.1933	3.3400
R_{max} (m)	3.3400	4.8319
τ_{min}	0.15415	0.35747
τ_{max}	0.35747	0.74815
Diagonal (m)	1.61	1.64
Width max. (m)	1.3259	0.9472
Height (m)	1.2471	1.4500
Segment area (m^2)	1.33	1.16

Table 3: Parameters of the mirror segments using the segmentation scheme F for the primary mirror. φ and τ are the two parameters used in the parametric equation of the mirrors. P1, P2 are respectively the inner and outer rings.

Mirror ring	S1	S2
Number of segments	8	16
φ_{min} (deg)	-22.5	-11.25
φ_{max} (deg)	22.5	11.25
R_{min} (m)	0.3945	1.5965
R_{max} (m)	1.5965	2.7083
τ_{min}	0.0435	0.4781
τ_{max}	0.4781	0.8148
Diagonal (m)	1.3467	1.3764
Width max. (m)	1.2219	1.0567
Height (m)	1.2320	1.0444
Segment area (m^2)	0.9398	0.9398

Table 4: Parameters of the mirror segments using the segmentation scheme J, for the secondary mirror. φ and τ are the two parameters used in the parametric equation of the mirrors. S1 and S2 are respectively the inner and outer rings.

1.6 Segment node positions

Each mirror segment is attached by 3 points on its surface, forming an equilateral triangle. These points are connected to 6 actuators on the back of the segment to create a Stewart platform (or hexapod). A single piece connects the other ends of the actuators with the mirror mechanical structure. This piece, called triangular mounting fixture in this document, has the shape of an equilateral triangle with the extremities holding the actuators and the center connected to the mechanical structure (Fig. 7).

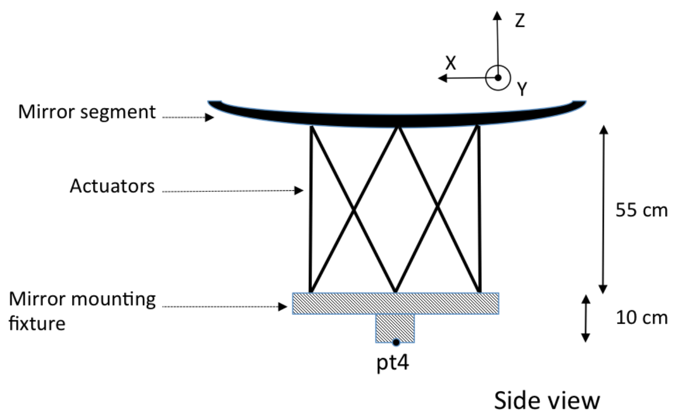

Figure 7: Representation of the mirror segment with the actuators and mirror mount. The total length (Stewart platform and triangular mounting fixture) along the Z axis is estimated to 65 cm.

The attached Excel file provides the positions in 3 dimensions of the 3 attachment points on the segment optical surface (pt1, pt2 and pt3) (Fig. 8) and the position of pt4, the center of the triangular mounting fixture, holding the actuators and the segment mirror (Fig. 7). These positions are calculated for the F (primary mirror) and J (secondary mirror) designs.

The attachment point positions on the mirror segments are the result of an optimization to equalize the torque due to the wind blowing on the mirror surface. A first geometry using two axes of rotation is presented Figure 8.

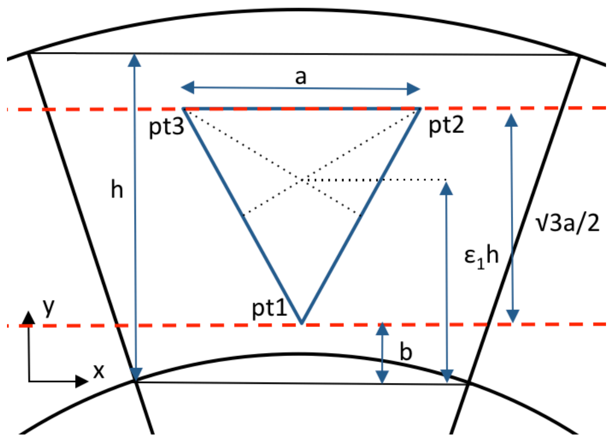

Figure 8: Representation of a mirror segment with the three attachment points (pt1, pt2, pt3) and the two axes of rotation (in red) used to calculate the torque due to the wind and the triangle center ($\varepsilon_1 h$).

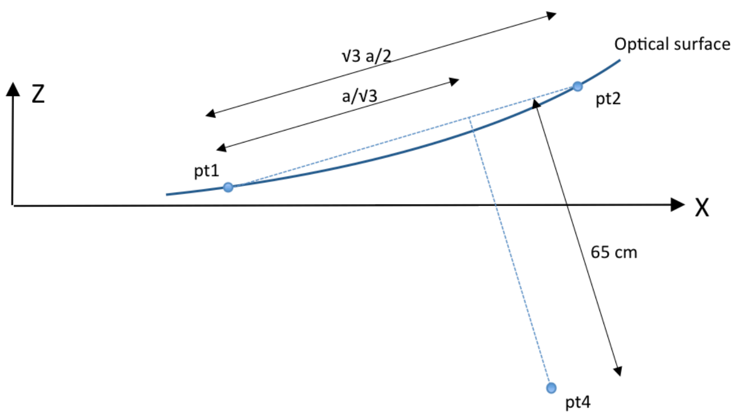

Figure 9: Representation of a mirror segment with two attachment points (pt1, pt2) on the optical surface and pt4, the center of the triangular mounting fixture, on the back of the segment.

The calculation of the torque, due to the wind around these two axis, gives :

$$\int (y-b)ds - 2N\frac{\sqrt{3}a}{2} = 0$$
$$\int \left(y-b-\frac{\sqrt{3}a}{2}\right)ds + N\frac{\sqrt{3}a}{2} = 0$$

with N the load on each point, $\frac{\sqrt{3}a}{2}$ the distance between the two axes and ds an element of surface along y.

Equations **Error! Reference source not found.** give the expression of the triangle parameters (a, b):

$$b+\frac{\sqrt{3}a}{3}=\frac{\int yds}{\int ds}$$

with $\int ds$ the total segment area.

If we introduce the triangle center $\varepsilon_1 h$ (Fig. 8), and if we assume that the triangle is equilateral, one obtain:

$$\varepsilon_1 h = b + \frac{\sqrt{3}a}{3} = \frac{\int y\, ds}{\int ds}$$

As we can see in the equation above, only the center of the triangle is constrained, but not its size.

A second estimation of the triangle center comes from the geometry presented Figure **Error! Reference source not found.** with a third axis of rotation.

Because pt1 and pt2 are at equal distance to this axis, the area on each side must be the same. This optimization leads to a second value of $\varepsilon_2 h$.

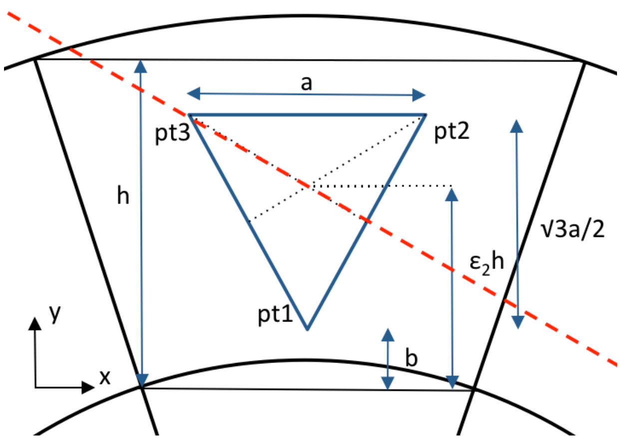

Figure 10: Representation of a mirror segment with the three attachment points (pt1, pt2, pt3) and the third axis of rotation (in red) used to calculate the torque due to the wind and the triangle center ($\varepsilon_2 h$).

The size of the triangle, formed by the three attachment points on the segment surface, is constant and equal to 55.4 cm. The area in the circumcircle contains around 1/3 of the total segment area and the attachment points are far enough to the edge to avoid any contact with the neighbor segments.

Because the triangles on each side of the Stewart platform have the same dimension, the constant distance between the attachment points authorizes the use of standard pieces (actuator length, mounting triangle) for all the telescope segments.

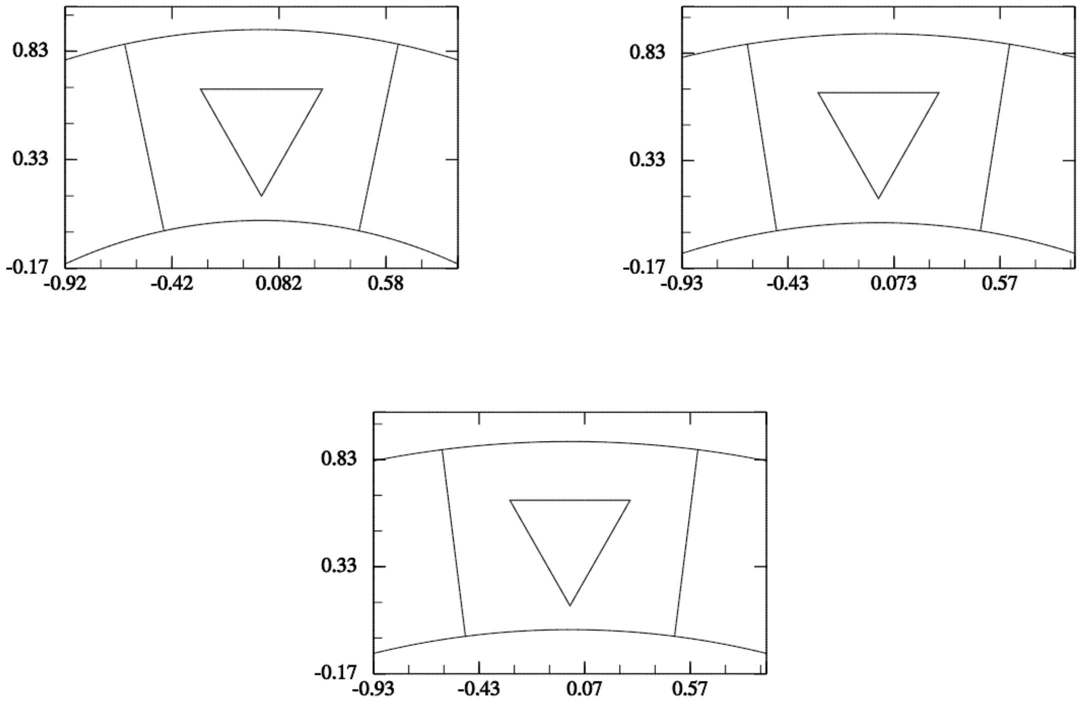

Figure 11 : P1 (inner), P2 (middle) and P3 (outer) segments of the D design for the primary mirror. The positions of the three attachment points on the mirror surface are represented by the equilateral triangle. The base of the triangle is 57 cm large.

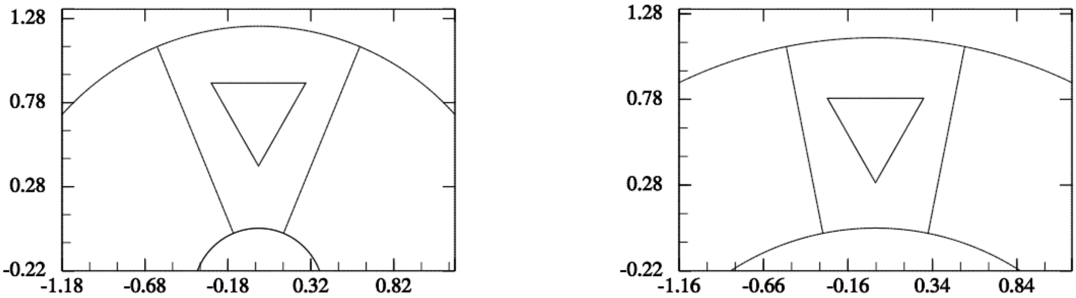

Figure 12: S1 (Inner) and S2 (outer) segments of the J design for the secondary mirror. The positions of the three attachment points on the mirror surface are represented by the equilateral triangle. The base of the triangle is 57 cm large.

1.7 References

Memo "Optical systems of Schwarzschild-Couder Telescope for CTA".